

PROCEEDINGS OF SPIE

Fifteenth International Conference on Correlation Optics

Oleg V. Angelsky
Editor

13–16 September 2021
Chernivtsi, Ukraine

Organized by
Chernivtsi National University (Ukraine)

Co-organized by
Research Institute of Zhejiang University-Taizhou (China)

Sponsored by
ICO – International Commission for Optics
Optica (formerly OSA), the Society Advancing Optics and Photonics Worldwide
Frontiers in Physics LTD
LTD "ROMA"
SKB "ELEKTRONMASH" (Ukraine)
Private Clinic of Eye Microsurgery "Your Vision" (Ukraine)
ARTON Company (Ukraine)

Co-sponsored by
SPIE

Published by
SPIE

Volume 12126

Proceedings of SPIE 0277-786X, V. 12126

SPIE is an international society advancing an interdisciplinary approach to the science and application of light.

Fifteenth International Conference on Correlation Optics, edited
by Oleg V. Angelsky, Proc. of SPIE Vol. 12126, 1212601
© 2021 SPIE · 0277-786X · doi: 10.1117/12.2626737

Proc. of SPIE Vol. 12126 1212601-1

The papers in this volume were part of the technical conference cited on the cover and title page. Papers were selected and subject to review by the editors and conference program committee. Some conference presentations may not be available for publication. Additional papers and presentation recordings may be available online in the SPIE Digital Library at SPIDigitalLibrary.org.

The papers reflect the work and thoughts of the authors and are published herein as submitted. The publisher is not responsible for the validity of the information or for any outcomes resulting from reliance thereon.

Please use the following format to cite material from these proceedings:

Author(s), "Title of Paper," in *Fifteenth International Conference on Correlation Optics*, edited by Oleg V. Angelsky, Proc. of SPIE 12126, Seven-digit Article CID Number (DD/MM/YYYY); (DOI URL).

ISSN: 0277-786X

ISSN: 1996-756X (electronic)

ISBN: 9781510651289

ISBN: 9781510651296 (electronic)

Published by

SPIE

P.O. Box 10, Bellingham, Washington 98227-0010 USA

Telephone +1 360 676 3290 (Pacific Time)

SPIE.org

Copyright © 2021 Society of Photo-Optical Instrumentation Engineers (SPIE).

Copying of material in this book for internal or personal use, or for the internal or personal use of specific clients, beyond the fair use provisions granted by the U.S. Copyright Law is authorized by SPIE subject to payment of fees. To obtain permission to use and share articles in this volume, visit Copyright Clearance Center at copyright.com. Other copying for republication, resale, advertising or promotion, or any form of systematic or multiple reproduction of any material in this book is prohibited except with permission in writing from the publisher.

Printed in the United States of America by Curran Associates, Inc., under license from SPIE.

Publication of record for individual papers is online in the SPIE Digital Library.

**SPIE. DIGITAL
LIBRARY**

SPIDigitalLibrary.org

Paper Numbering: A unique citation identifier (CID) number is assigned to each article in the Proceedings of SPIE at the time of publication. Utilization of CIDs allows articles to be fully citable as soon as they are published online, and connects the same identifier to all online and print versions of the publication. SPIE uses a seven-digit CID article numbering system structured as follows:

- The first five digits correspond to the SPIE volume number.
- The last two digits indicate publication order within the volume using a Base 36 numbering system employing both numerals and letters. These two-number sets start with 00, 01, 02, 03, 04, 05, 06, 07, 08, 09, 0A, 0B ... 0Z, followed by 10-1Z, 20-2Z, etc. The CID Number appears on each page of the manuscript.

- 12126 1M **Fourier energy analysis of Kikuchi patterns for investigation of defect system of diamond crystals** [12126-67]
- 12126 1N **Stabilizing effect of random phase diffuser against wavefront distortions to the intensity distribution formed by Fourier hologram** [12126-70]
- 12126 1O **Registration of three-dimensional holograms based on microsystems "Core CaF₂ –Shell AgBr"** [12126-71]
- 12126 1P **Extraordinary transverse spin: hidden vorticity of the energy flow and momentum distributions in propagating light fields** [12126-72]
- 12126 1Q **Energy and momentum of the surface plasmon-polariton supported by a thin metal film** [12126-73]
- 12126 1R **Optical control of colour deviation due to ink showing through on the banknote reverse on multicolored watermarks** [12126-74]
- 12126 1S **Electrical properties of photosensitive ZnO/Si heterostructure depending on temperature** [12126-75]
- 12126 1T **Evidence for the need to update the definition of the BRDF: spectral considerations** [12126-76]
- 12126 1U **UV sensitive heterojunction ZnCoO/n-GaP prepared by spray pyrolysis** [12126-77]
- 12126 1V **Influence of chromium sublayer on silicon P-I-N photodiodes responsivity** [12126-78]
- 12126 1W **Dynamic interferometry method for measuring wavelength** [12126-79]
- 12126 1X **Measurement of parameters of optically transparent films** [12126-80]
- 12126 1Y **Optical transfer matrix: matrix correlation as frequency domain analysis of polarization imaging system (Invited Paper)** [12126-82]
- 12126 1Z **Algorithm for diagnosing pancreatic endocrine dysfunction based on biochemical and laser polarimetric parameters** [12126-83]
- 12126 20 **The effect of photonic correction on the optical and photoelectric characteristics of the In₄Se₃, In₄Te₃ and GaP epitaxial structures** [12126-84]
- 12126 21 **Forensic medical assessment of cerebral infarction, hemorrhagic hemorrhages of traumatic genesis and determination of the duration of their formation methods of spectral-selective laser-induced direct polarization-phase tomography** [12126-86]
- 12126 22 **Polarization mapping of laser-induced monospectral fields of optically anisotropic fluorophores in forensic diagnostics of the age of the formation of damage to human organs** [12126-87]
- 12126 23 **Mueller-matrix microscopy of laser-induced monochromatic fluorescent fields of preparations of human internal organs and histological diagnostics of the time of age of damage formation** [12126-89]

Forensic medical assessment of cerebral infarction, hemorrhagic hemorrhages of traumatic genesis and determination of the duration of their formation methods of spectral-selective laser-induced direct polarization-phase tomography

M.S. Garazdyuk¹, V.T. Bachinsky¹, Yu.A. Ushenko², P.A. Gorodenskiy², V.K. Gantuyuk²,
M.M. Slyotov², I.V. Fesiv², Hulei¹ L, Oliinyk¹ I.

¹ Bukovinian State Medical University, Chernivtsi, Ukraine

²Chernivtsi National University, Chernivtsi, Ukraine

ABSTRACT

The structural-logical diagram and research design by the methods of polarization-phase tomography of linear dichroism of the polycrystalline structure [1-5] of histological sections of the brain are presented. Differential diagnosis of the formation of hemorrhages of traumatic genesis, cerebral infarction of ischemic and hemorrhagic genesis by the method of differential Mueller-matrix mapping of amplitude anisotropy - linear dichroism maps (ALD) of histological brain sections and operational characteristics of the method of their statistical analysis.

Differential diagnosis of the prescription of the formation of hemorrhages of traumatic genesis, cerebral infarction, ischemic and hemorrhagic genesis by the method of differential Mueller-matrix mapping of amplitude anisotropy - temporal dynamics of changes in the statistical structure of ALD maps of histological brain sections.

Keywords: polarization, optical anisotropy, linear dichroism, Mueller's matrix, statistical moments of the 1st-4th orders, hemorrhages of traumatic origin, cerebral infarction of ischemic and hemorrhagic genesis.

1. STRUCTURAL AND LOGICAL DIAGRAM OF POLARIZATION-PHASE TOMOGRAPHY OF THE POLYCRYSTALLINE STRUCTURE OF HISTOLOGICAL SECTIONS OF BRAIN

Histological sections of the brain of the deceased			
Control group deceased (group 1)	Hemorrhage of traumatic genesis (group 2)	Cerebral infarction of ischemic genesis (group 3)	Cerebral infarction of hemorrhagic genesis (group 4)
Mueller-matrix mapping of maps of elements of 1st order differential matrix [6,7]			
Algorithms for reconstructing the distributions of average values of parameters of amplitude anisotropy			
Linear dichroism maps (ALD)			
Statistical analysis of ALD maps			
Average values and standard deviations of the magnitude of the statistical moments of the 1st - 4th orders, which characterize the coordinate distributions of the ALD value			
Criteria for differential diagnosis of samples of histological sections of the brain of the deceased from groups 1 - 4			
Time dynamics of changes in the value of statistical moments of the 1st - 4th orders, which characterize the coordinate distributions of the ALD value			
Duration of formation of hemorrhages of traumatic genesis, cerebral infarction of ischemic and hemorrhagic genesis by methods of polarization-phase tomography [8-12]			

Fig. 1. Structural and logical diagram of polarization-phase tomography of histological sections of the brain

2. DIFFERENTIAL DIAGNOSIS OF THE FORMATION OF HEMORRHAGES OF TRAUMATIC GENESIS, CEREBRAL INFARCTION ISCHEMIC AND HEMORRHAGIC GENESIS BY THE METHOD OF POLARIZATION-PHASE REPRODUCTION OF LINEAR DICHROISM

A series of fragments in Fig. 2 shows the results of studying the coordinate (fragments (1), (3), (5), (7)) and histograms (fragments (2), (4), (6), (8)) distributions of the linear dichroism value of fibrillar networks of the nervous brain tissue with various types of pathology.

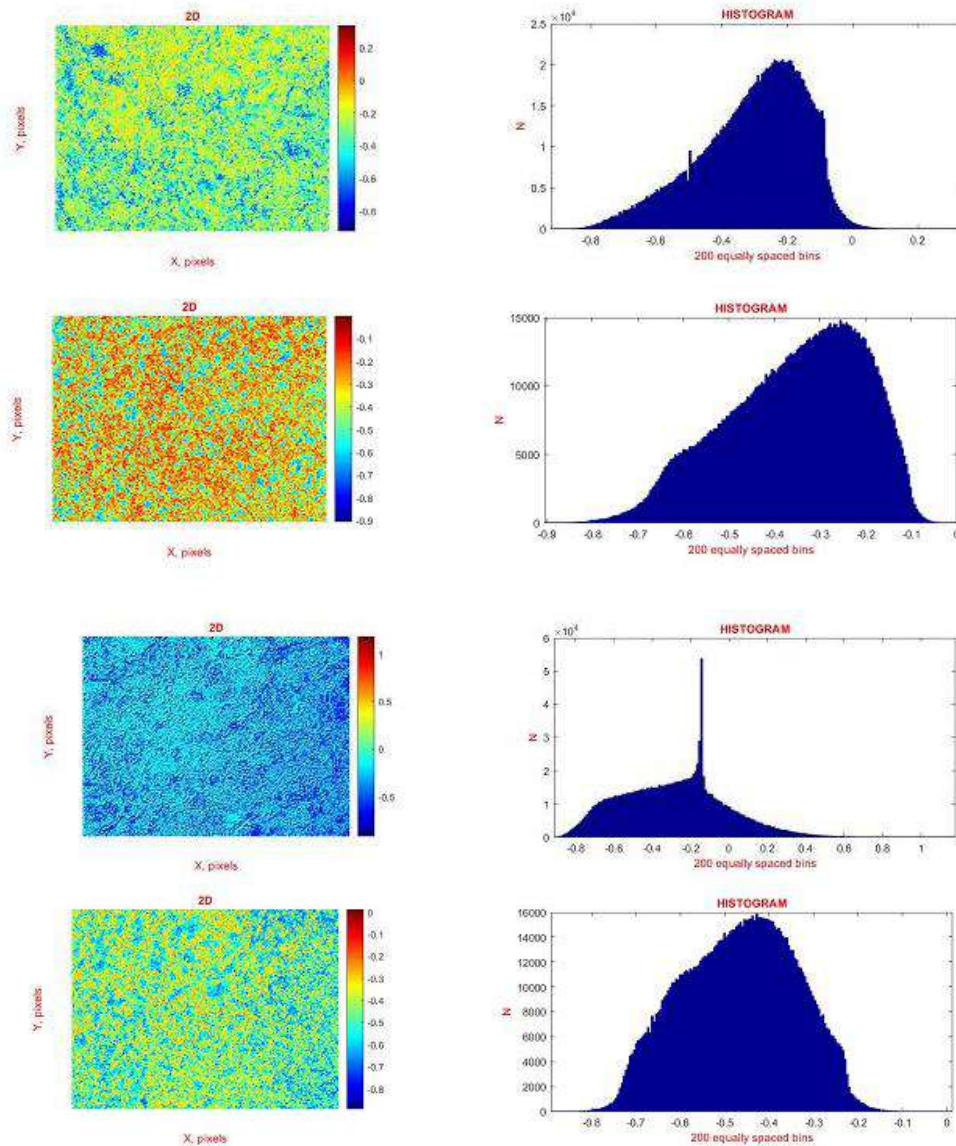


Fig. 2. Maps ((1), (2), (3), (4)) and histograms ((4), (5), (6), (7)) of the distribution of the ALD value of histological sections of the brain of the deceased from group 1 ((1), (5)), group 2 ((2), (6)), group 3 ((3), (7)) and group 4 ((4), (8)).

Analysis of polarization-reconstructed ALD maps revealed:

- individual topographic structure of all ALD maps of histological sections of the nervous tissue of the brain of the deceased from groups 1 - 4 (Fig. 2, fragments (1), (3), (5), (7));
- The histograms characterizing the distributions of the linear dichroism value of the fibrillar networks of the brain nervous tissue samples from the control 1 and research groups 2 - 4 are characterized by maximum differences in the average value SM_1 , the spread of random values (dispersion SM_2), significant skewness (SM_3) and sharpness (kurtosis SM_4) of the peak (Fig. 5.4, fragments (2), (4), (6), (8)).

Table 1 presents the data of the statistical analysis of ALD maps - the mean values and errors ($\pm\Omega$) for determining the set of statistical moments of the 1st - 4th orders $SM_{i=1-4}$, characterizing the distributions of the linear dichroism value of the nervous tissue of the brain.

Table 1 Statistical moments of the 1st - 4th orders, characterizing the distributions of the ALD value of histological sections of the brain of groups 1 – 4

Parameters	Group 1	Group 2	Group 3	Group 4
SM_1	$0,18 \pm 0,008$	$0,24 \pm 0,011$	$0,31 \pm 0,014$	$0,39 \pm 0,017$
p_1		$p < 0,05$	$p < 0,05$	$p < 0,05$
p_2		$p < 0,05$		$p < 0,05$
p_3		$p < 0,05$	$p < 0,05$	
p_4		$p < 0,05$		
SM_2	$0,33 \pm 0,015$	$0,39 \pm 0,018$	$0,45 \pm 0,021$	$0,51 \pm 0,023$
p_1		$p < 0,05$	$p < 0,05$	$p < 0,05$
p_2		$p < 0,05$		$p < 0,05$
p_3		$p < 0,05$	$p < 0,05$	
p_4		$p < 0,05$		
SM_3	$0,65 \pm 0,031$	$0,77 \pm 0,035$	$0,91 \pm 0,042$	$1,11 \pm 0,052$
p_1		$p < 0,05$	$p < 0,05$	$p < 0,05$
p_2		$p < 0,05$		$p < 0,05$
p_3		$p < 0,05$	$p < 0,05$	
p_4		$p < 0,05$		
SM_4	$0,53 \pm 0,023$	$0,91 \pm 0,041$	$0,79 \pm 0,036$	$1,18 \pm 0,051$
p_1		$p < 0,05$	$p < 0,05$	$p < 0,05$
p_2		$p < 0,05$		$p < 0,05$
p_3		$p < 0,05$	$p < 0,05$	
p_4		$p < 0,05$		

The results of statistical analysis of the data of polarization-phase tomography of linear dichroism maps shown in Table 1 illustrate the statistically significant difference ($p_{i=1;2;3;4} < 0,05$) between the mean values of all statistical moments of the 1st - 4th orders, which are determined within all representative samples of histological sections of the brain.

3. OPERATIONAL CHARACTERISTICS OF THE METHOD OF STATISTICAL ANALYSIS OF ALD MAPS OF HISTOLOGICAL BRAIN SECTIONS

By tomographic reproduction of ALD maps, the following parameters of the operational characteristics of force (sensitivity, specificity and balanced accuracy) of this method of reconstruction of the polycrystalline component of the nervous tissue of the brain were established:

- good (average SM_1 and dispersion SM_2 - 85% - 92% spread of ALD values) and excellent (statistical moments of higher orders $SM_3; SM_4$, which determine the skewness and sharpness of the peak of ALD distributions - 98% - 100%) balanced accuracy of differentiation of a set of representative samples of histological sections of the brain of group "1" - "2 + 3 + 4";
- satisfactory (average SM_1 and dispersion SM_2 - 80% - 84% of the spread of ALD values) and excellent ($SM_3; SM_4$ - 95% - 97%) balanced accuracy of intergroup differentiation of histological sections of the brain of group "2" (traumatic hemorrhage) - "4" (cerebral infarction of ischemic genesis), as well as intergroup differentiation of histological sections of the brain of group "2" (traumatic hemorrhage) - "3" (cerebral infarction of hemorrhagic genesis);
- good ($SM_{3,4}$ - 90% - 94%) balanced accuracy of intergroup differentiation of histological sections of the brain of group "3" - "4".

Table2 Specificity, sensitivity, accuracy of the method of statistical analysis of ALD maps of histological brain sections

Groups "1 - 2+3+4"			
Parameters	Sensitivity, Se, %	Specificity, Sp, %	Accuracy, Ac, %
SM_1	a = 86; b = 14	c = 85; d = 15	n = 100
	86	85	85,5
SM_2	a = 92; b = 8	c = 90; d = 10	n = 100
	92	90	91
SM_3	a = 100; b = 0	c = 98; d = 2	n = 100
	100	98	99
SM_4	a = 100; b = 0	c = 98; d = 2	n = 100
	100	98	99
Groups "2 - 3"			
Parameters	Sensitivity, Se, %	Specificity, Sp, %	Accuracy, Ac, %
SM_1	a = 82; b = 18	c = 80; d = 20	n = 100
	82	80	81
SM_2	a = 84; b = 16	c = 81; d = 19	n = 100
	84	81	82,5
SM_3	a = 96; b = 4	c = 95; d = 5	n = 100
	96	95	95,5
SM_4	a = 97; b = 3	c = 95; d = 5	n = 100
	97	95	96
Groups "2 - 4"			
Parameters	Sensitivity, Se, %	Specificity, Sp, %	Accuracy, Ac, %
SM_1	a = 83; b = 17	c = 81; d = 19	n = 100
	83	81	82
SM_2	a = 85; b = 15	c = 83; d = 17	n = 100

	85	83	84
SM ₃	a = 97; b = 3	c = 95; d = 5	n = 100
	97	95	96
SM ₄	a = 96; b = 4	c = 95; d = 5	n = 100
	96	95	95,5
Groups "3 - 4"			
Parameters	Sensitivity, Se, %	Specificity, Sp, %	Accuracy, Ac, %
SM ₁	a = 80; b = 20	c = 78; d = 22	n = 100
	80	78	79
SM ₂	a = 78; b = 22	c = 77; d = 23	n = 100
	78	77	77,5
SM ₃	a = 92; b = 8	c = 90; d = 10	n = 100
	92	90	91
SM ₄	a = 94; b = 16	c = 92; d = 8	n = 100
	94	92	93

4. DIFFERENTIAL DIAGNOSIS OF THE AGE OF THE FORMATION OF HEMORRHAGES OF TRAUMATIC GENESIS, CEREBRAL INFARCTION OF ISCHEMIC AND HEMORRHAGIC GENESIS BY THE METHOD OF REPRODUCING ALD DISTRIBUTIONS

In fig. 3 - fig. 5 shows maps (fragments (1), (3)) and histograms of distributions (fragments (2), (4)) of the magnitude of circular birefringence of samples of histological sections of the nervous tissue of the brain of the deceased of all groups.

Tables 3 - 5 show the results of a statistical analysis of temporary changes in necrotic changes in the structure of ALD maps of the nervous tissue of the brain of the deceased within the representative samples of samples from group 2 (table 3), group 3 (table 4) and group 4 (table 5) with different AOD (antiquity of onset of death).

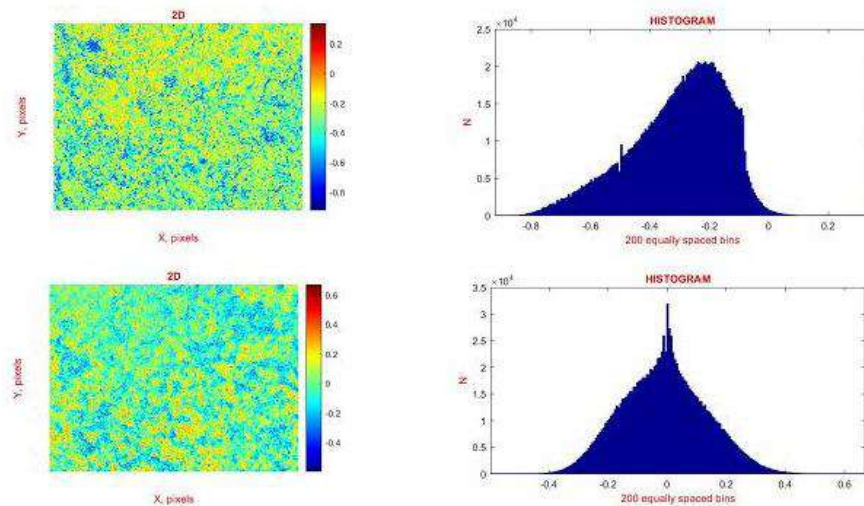


Fig. 3. Maps ((1), (2)) and histograms ((3), (4)) of the distribution of the ALD value of histological sections of the brain of the deceased from group 2 for AOD 6 hours. ((1), (3)) and AOD 24 hours ((2), (4)).

Table 3 Time dynamics of changes in the statistical moments of the 1st - 4th orders characterizing the distributions of the ALD value of histological brain sections of the deceased from group 2

T, hours	6	12	18	24	48
SM ₁	0,24 ± 0,008	0,22 ± 0,007	0,205 ± 0,006	0,19 ± 0,005	0,16 ± 0,005
p	p < 0,05				
SM ₂	0,41 ± 0,014	0,37 ± 0,013	0,35 ± 0,013	0,33 ± 0,012	0,25 ± 0,01
p	p < 0,05				
SM ₃	0,91 ± 0,034	1,39 ± 0,054	1,63 ± 0,072	1,87 ± 0,088	2,83 ± 0,11
p	p < 0,05				
SM ₄	0,78 ± 0,031	1,33 ± 0,059	1,58 ± 0,065	2,79 ± 0,11	2,91 ± 0,12
p	p < 0,05				
T, hours	72	96	120	144	168
SM ₁	0,11 ± 0,004	0,08 ± 0,003	0,09 ± 0,004	0,08 ± 0,003	0,07 ± 0,003
p	p < 0,05		p > 0,05		
SM ₂	0,17 ± 0,006	0,11 ± 0,004	0,12 ± 0,004	0,11 ± 0,004	0,12 ± 0,004
p	p < 0,05		p > 0,05		
SM ₃	3,73 ± 0,31	4,51 ± 0,32	4,66 ± 0,32	4,12 ± 0,31	4,39 ± 0,31
p	p < 0,05		p > 0,05		
SM ₄	3,98 ± 0,23	4,71 ± 0,25	4,88 ± 0,26	4,56 ± 0,22	4,39 ± 0,21
p	p < 0,05		p > 0,05		

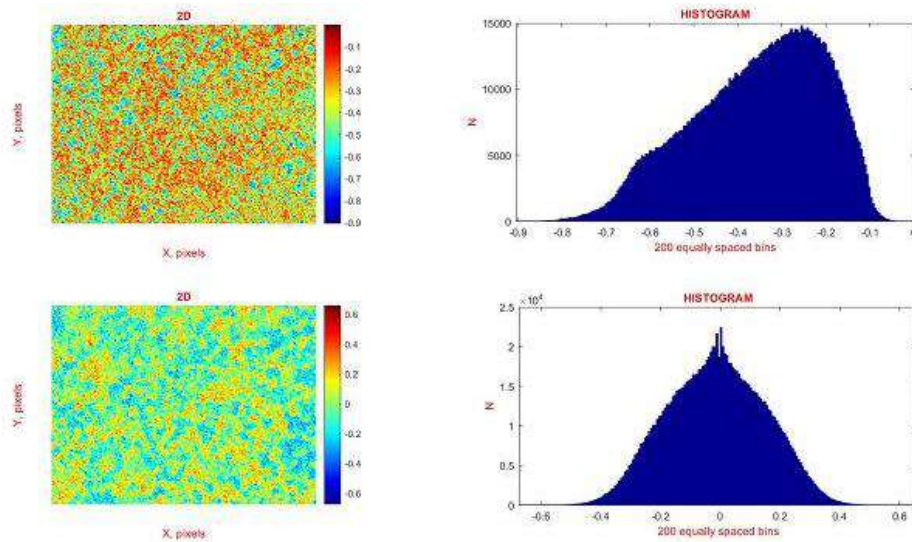


Fig. 4. Maps ((1), (2)) and histograms ((3), (4)) of the distribution of the ALD value of histological sections of the brain of the deceased from group 3 for AOD 6 hours. ((1), (3)) and AOD 24 hours ((2), (4)).

Table 4 Time dynamics of changes in the statistical moments of the 1st - 4th orders, characterizing the distribution of the ALD value of histological brain sections of the deceased from group 3

T, hours	6	12	18	24	48
SM ₁	0,15 ±	0,137 ±	0,13 ±	0,12 ±	0,1 ±
p	p < 0,05				
SM ₂	0,31 ±	0,28 ±	0,26 ±	0,25 ±	0,205 ±
p	p < 0,05				
SM ₃	0,71 ±	1,06 ±	1,23 ±	1,41 ±	2,11 ±
p	p < 0,05				
SM ₄	0,63 ±	1,06 ±	1,27 ±	1,48 ±	2,03 ±
p	p < 0,05				
T, hours	72	96	120	144	168
SM ₁	0,07 ±	0,05 ±	0,06 ±	0,05 ±	0,04 ±
p	p < 0,05		p > 0,05		
SM ₂	0,13 ±	0,08 ±	0,09 ±	0,08 ±	0,07 ±
p	p < 0,05		p > 0,05		
SM ₃	2,79 ±	3,35 ±	3,44 ±	3,13 ±	3,27 ±
p	p < 0,05		p > 0,05		
SM ₄	3,19 ±	3,81 ±	3,99 ±	3,73 ±	3,88 ±
p	p < 0,05		p > 0,05		

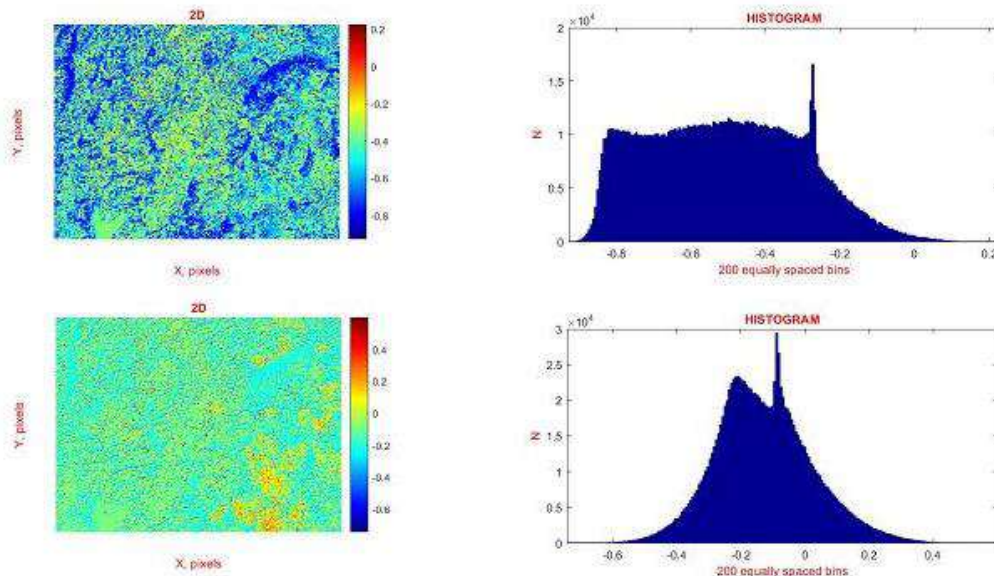


Fig. 5. Maps ((1), (2)) and histograms ((3), (4)) of the distribution of the ALD value of histological sections of the brain of the deceased from group 4 for AOD 6 hours. ((1), (3)) and AOD 24 hours ((2), (4)).

Table 5 Time dynamics of changes in the statistical moments of the 1st - 4th orders, characterizing the distribution of the ALD value of histological brain sections of the deceased from group 4

T, hours	6	12	18	24	48
SM ₁	0,21 ± 0,006	0,192 ± 0,005	0,18 ± 0,005	0,17 ± 0,004	0,14 ± 0,003
p	p < 0,05				
SM ₂	0,36 ± 0,009	0,33 ± 0,008	0,31 ± 0,007	0,285 ± 0,006	0,23 ± 0,005
p	p < 0,05				
SM ₃	0,69 ± 0,021	1,09 ± 0,029	1,31 ± 0,033	1,52 ± 0,055	2,34 ± 0,16
p	p < 0,05				
SM ₄	0,83 ± 0,026	1,36 ± 0,034	1,63 ± 0,043	1,89 ± 0,049	2,96 ± 0,17
p	p < 0,05				
T, hours	72	96	120	144	168
SM ₁	0,095 ± 0,003	0,07 ± 0,0025	0,08 ± 0,003	0,07 ± 0,003	0,09 ± 0,004
p	p < 0,05		p > 0,05		
SM ₂	0,16 ± 0,004	0,09 ± 0,003	0,1 ± 0,004	0,09 ± 0,003	0,08 ± 0,003
p	p < 0,05		p > 0,05		
SM ₃	3,17 ± 0,16	3,51 ± 0,17	3,57 ± 0,17	3,43 ± 0,16	3,51 ± 0,17
p	p < 0,05		p > 0,05		
SM ₄	4,03 ± 0,19	4,88 ± 0,21	4,99 ± 0,22	4,76 ± 0,21	4,94 ± 0,22
p	p < 0,05		p > 0,05		

From the analysis of the results of statistical processing of the topographic structure of tomograms of linear dichroism of fibrillar networks of histological sections of the brain (Fig. 3 - Fig. 5) of the deceased from all groups, one can see a large temporal dynamics of necrotic destruction of the nervous tissue. In accordance with this, there is a faster temporal decrease in the absolute values and the range of scatter of the linear dichroism value with increasing AOD time (Fig. 3 - Fig. 5, fragments (2), (4)).

The following regularities of the scenario of temporary changes in the topographic structure of the ALD maps have been established:

- an increase in the magnitude of the range of temporal linear changes in the values of statistical moments of the 1st - 4th orders, characterizing the distributions of the magnitude of the linear dichroism of fibrillar networks of histological sections of the nervous tissue of the brain of the deceased from all groups up to 24 hours;
- the accuracy of the AOD determination is 30 min. ± 5 min.

CONCLUSIONS

1. The design of forensic differentiation of cases of cerebral infarction, hemorrhagic hemorrhages of traumatic genesis and determination of the age of their formation by means of experimental testing of methods of polarization-phase tomography of optical anisotropy, investigated on the basis of the developed structural-logical scheme, has been substantiated.

2. The following parameters of the strength of the method of polarization-phase tomography were experimentally established:

- Linear dichroism - good (SM_1 and SM_2 - 85% - 92%) and excellent (SM_3 ; SM_4 - 98% - 100%) balanced accuracy of differentiation of a set of representative samples of histological brain sections of group "1" - "2 + 3 + 4";

satisfactory (SM_1 and SM_2 - 80% - 84%) and excellent ($SM_3; SM_4$ - 95% - 97%) balanced accuracy of intergroup differentiation of histological sections of the brain of group "2" - "4", as well as intergroup differentiation of histological sections of the brain of group "2" - "3"; good ($SM_{3;4}$ - 90% - 94%) balanced accuracy of intergroup differentiation of histological sections of the brain of the group "3" - "4";

3. By temporarily monitoring the change in the magnitude of the statistical moments of the 1st - 4th orders, which characterize the polarization-reproduced maps of the set of mechanisms of optical anisotropy of the polycrystalline structure of the nervous tissue, the following parameters of the differential determination of the duration of the formation of cases of cerebral infarction, hemorrhagic hemorrhages of traumatic genesis were determined:

- tomography of the distributions of the linear dichroism value of histological sections of the brain – AOD 24 hours, accuracy 30 min. \pm 5 min.

FUNDING

Current research supported by the National Research Foundation of Ukraine (Project 2020.02/0061)

REFERENCES

- [1] S. Alali et al., "Quantitative correlation between light depolarization and transport albedo of various porcine tissues," J. Biomed. Opt. 17(4), 045004 (2012).
- [2] A. Pierangelo et al., "Multispectral Mueller polarimetric imaging detecting residual cancer and cancer regression after neoadjuvant treatment for colorectal carcinomas," J. Biomed. Opt. 18(4), 046014 (2013).
- [3] E. Du et al., "Mueller matrix polarimetry for differentiating characteristic features of cancerous tissues," J. Biomed. Opt. 19(7), 076013 (2014).
- [4] A. Doronin, C. Macdonald, and I. Meglinski, "Propagation of coherent polarized light in highly scattering turbid media," J. Biomed. Opt. 19(2), 025005 (2014).
- [5] B. Kunnen et al., "Application of circularly polarized light for non-invasive diagnosis of cancerous tissues and turbid tissue-like scattering media," J. Biophotonics 8(4), 317–323 (2015).
- [6] Ushenko, V.O., Trifonyuk, L., Ushenko, Y.A., Dubolazov, O.V., Gorsky, M.P., Ushenko, A.G. Polarization singularity analysis of Mueller-matrix invariants of optical anisotropy of biological tissues samples in cancer diagnostics (2021) Journal of Optics (United Kingdom), 23 (6), 064004.
- [7] Meglinski, I., Trifonyuk, L., Bachinsky, V., Vanchulyak, O., Bodnar, B., Sidor, M., Dubolazov, O., Ushenko, A., Ushenko, Y., Soltys, I.V., Bykov, A., Hogan, B., Novikova, T. Polarization Correlometry of Microscopic Images of Polycrystalline Networks Biological Layer (2021) SpringerBriefs in Applied Sciences and Technology, pp. 61-73.
- [8] Angelsky, O.V., Bekshaev, A.Y., Dragan, G.S., Maksimyak, P.P., Zenkova, C.Y., Zheng, J. Structured Light Control and Diagnostics Using Optical Crystals (2021) Frontiers in Physics, 9, 715045.
- [9] Angelsky, O.V., Bekshaev, A.Y., Hanson, S.G., Zenkova, C.Y., Mokhun, I.I., Jun, Z. Structured Light: Ideas and Concepts (2020) Frontiers in Physics, 8, 114
- [10] Ushenko, A.G. Laser Polarimetry of Polarization-Phase Statistical Moments of the Object Field of Optically Anisotropic Scattering Layers (2001) Optics and Spectroscopy (English translation of Optika i Spektroskopiya), 91 (2), pp. 313-316
- [11] Angelsky, O.V., Maksimyak, P.P. Optical diagnostics of slightly rough surfaces (1992) Applied Optics, 31 (1), pp. 140-143
- [12] Angelsky, O.V., Zenkova, C.Y., Hanson, S.G., Zheng, J. Extraordinary Manifestation of Evanescent Wave in Biomedical Application (2020) Frontiers in Physics, 8, 159.
- [13] Angelsky, O.V., Hanson, S.G., Maksimyak, A.P., Maksimyak, P.P. On the feasibility for determining the amplitude zeroes in polychromatic fields (2005) Optics Express, 13 (12), pp. 4396-4405
- [14] Ushenko, A.G., Burkovets, D.N., Ushenko, Yu.A. Polarization-Phase Mapping and Reconstruction of Biological Tissue Architectonics during Diagnosis of Pathological Lesions (2002) Optics and Spectroscopy (English translation of Optika i Spektroskopiya), 93 (3), pp. 449-456.
- [15] Ushenko, A.G. Laser Polarimetry of Polarization-Phase Statistical Moments of the Object Field of Optically Anisotropic Scattering Layers (2001) Optics and Spectroscopy (English translation of Optika i Spektroskopiya), 91 (2), pp. 313-316.

Polarization mapping of laser-induced monospectral fields of optically anisotropic fluorophores in forensic diagnostics of the age of the formation of damage to human organs

Litvinenko¹ A., Tryfonyuk² L., Pavlyukovich¹ O., Pavlyukovich¹ N., Stashkevich³ A.T.,
Olar⁴ O., Kurek⁴ O.I., Tkachuk⁴ V.I.

¹Bukovinian State Medical University, Chernivtsi, Ukraine

²Rivne State Medical Hospital, Rivne, Ukraine

³The Institute of Traumatology and Orthopedics by NAMS of Ukraine, Kyiv, Ukraine

⁴Chernivtsi National University, Chernivtsi, Ukraine

cablaze9@gmail.com

ABSTRACT

The paper presents the results of experimental testing of methods for azimuthal-invariant polarization mapping of laser-induced microscopic images of fluorophores in histological sections of the liver of deceased; time monitoring of changes in the magnitude of statistical moments of the 1st - 4th orders characterizing the distributions of the azimuth and ellipticity of polarization of microscopic images of histological sections of the liver with different age of damage; determination of the diagnostic efficiency (time interval and accuracy) of establishing the age of damage to human internal organs by digital histological methods of mapping maps of azimuth and ellipticity of polarization of microscopic images of samples of histological sections of the brain, liver and kidney, as well as myocardium and lung tissue.

Keywords: polarization, azimuth, ellipticity, microscopic image, statistical moments of the 1st - 4th orders, histological sections, biological tissues, damages

1. INTRODUCTION

The methodology and technique of polarization mapping of microscopic images of biological preparations are presented in detail and comprehensively in numerous publications of the scientific schools [1-8].

The obtained results of polarization mapping revealed information (diagnostic) relationships between:

- maps of polarization azimuth and concentration of optically active molecular compounds (fluorophores) of biological tissues and fluids of human organs;
- maps of ellipticity of polarization and the degree of ordering (crystallization) of fibrillar networks of biological preparations.

However, at present, these digital methods of polarizing microscopy are practically absent in histological studies for determining the age of damage to human internal organs..

The aim of the study is to develop a set of objective forensic criteria for expanding the functionality and improving the accuracy of establishing the age of damage to human internal organs according to the data of a multiparametric digital histological study of liver tissue through the integrated use of polarization mapping of the polycrystalline structure of fluorophores of prototypes based on a statistical analysis of the temporal dynamics of their change [9-15].

2. MATERIALS AND METHODS

The following groups were formed (control group with those who died from coronary artery disease and experienced with different age of damage) of experimental samples of histological sections of internal organs (brain, liver, kidney, as well as myocardium and lung tissue) of a person.